D 00012948

Advanced Accelerator Applications	**DOCUMENT RELEASE AUTHORIZATION**	ARGONNE NATIONAL LABORATORY · UNIVERSITY OF CHICAGO

Argonne National Laboratory
9700 South Cass Avenue
Argonne, IL 60439

ANL AAA Document Number:	ANL-AAA-018	Release Date:	6/28/2002

Title:	Assessment of CORAIL-Pu Multi-Recycling in PWRs

Author(s):	Taek K. Kim

Approval for Release

Approved by:			Date
Principal Author:	Taek K. Kim		
ANL WBS Level 2 Manager:	Robert N. Hill		
ANL Program Manager:	Phillip J. Finck		

2008000 2235

1. Abstract

Recently, the French CEA proposed the use of the so-called CORAIL assembly design for stabilizing the production of plutonium in a PWR.[1] One of the attractive features of the CORAIL concept is that it makes use of a retrofittable PWR fuel assembly design without adversely affecting core safety and operational parameters or fuel cycle infrastructures (i.e., uranium enrichment and plutonium production capabilities). In previous work[2], performance parameters and reactivity coefficients for the CORAIL assembly were evaluated for a single startup reactor cycle. The current report summarizes the methodologies used in this study and the evaluation of the CORAIL assembly as part of a sustainable nuclear enterprise with multi-recycling of plutonium.

The CORAIL assembly employs a standard 17x17 PWR fuel assembly with a heterogeneous loading of UO_2 and MOX fuel pins. In a 3 batch, 15,000 MWD/t cycle length fuel management scheme, the plutonium content in the MOX pins reaches an equilibrium of around 8%, with a uranium enrichment in the UO_2 pins of around 4.8%. At equilibrium, the Pu is "stabilized", such that there is no *net* production of Pu in the reactor cycle. Also, the reactivity coefficients of a core fully loaded with CORAIL assemblies do not show any significant differences to those of a reference UO_2 core.

It is important to recognize that the fuel cycle studies described in this report are based on a recycle process employing plutonium separation. In future work, the performance impact for recycle of all transuranics (no plutonium separation) in the CORAIL concept will be evaluated in a similar manner.

2. Characteristics of the CORAIL Assembly

As shown in Figure 2.1, one of the distinguishing features of the CORAIL assembly proposed by CEA is its heterogeneous fuel pin configuration. It contains 180 UO_2 fuel pins in the interior and 84 MOX fuel pins in the peripheral region in order to reduce the hot-channel factor (the highest normalized pin power in the assembly) and maintain reactivity coefficients similar to those in a typical UO_2 fuel assembly. If the MOX pins are located near the guide tubes or in the interior of the assembly, the relatively large fission cross sections of the Pu isotopes may increase the hot-channel factor to an unacceptable level. It has been shown that a core loading of 20-50% homogeneous MOX fuel assemblies can be tolerated without violating safety criteria.[3] For a full core loading of CORAIL assemblies, the fraction of MOX pins in the core (32%) falls within that range.
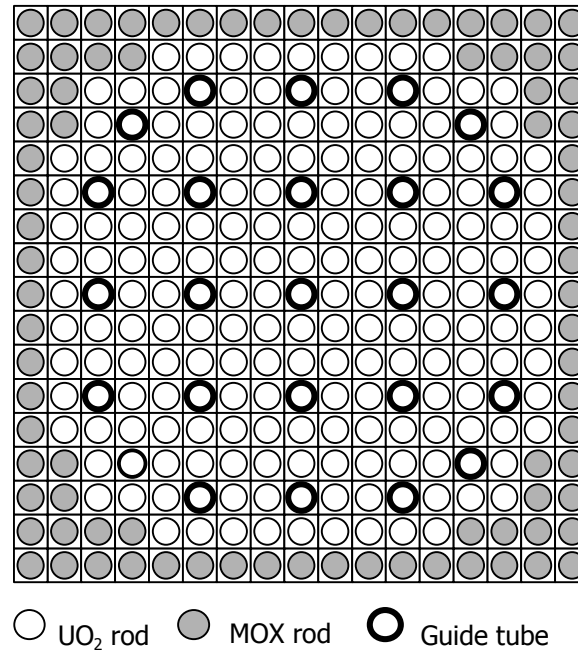

Figure 2.1. Heterogeneous Pin Loading Pattern in the CORAIL Assembly.

The CORAIL assembly design parameters utilized in this study were derived from a standard 17x17 Westinghouse assembly[4] and data provided in Reference 1. Table 2.1 compares the main design parameters of this assembly design and those used in the CEA studies. In spite of the differences in the pellet radius and density, the total heavy metal mass in the each assembly was conserved by adjusting the density of fuel pellet.

Table 2.1. Main Design Parameters of the Westinghouse and the CEA Assembly Designs.

	Westinghouse 17x17	CEA 17x17
Assembly geometry	17x17	17x17
No of rods (UO$_2$/MOX)	180 / 84	180 / 84
Mass of heavy metal, kg [a] (UO$_2$/MOX)	365 / 170	365 / 170
Assembly pitch, cm	21.5	21.6112
Active height, cm	427.0 [a]	427.0 [a]
Assembly gap, cm	0.08	0.1559
Fuel pitch, cm	1.2600	1.262082
Cladding outer radius, cm	0.4750	0.474364
Cladding thickness, cm	0.0572	N/A
Pellet-cladding gap, cm	0.0083	N/A
Pellet radius, cm	0.4095	0.41266
Cladding material	Zr-4	N/A
Cladding density, g/cm^3	6.5	6.49012
Guide tube inner radius, cm	0.5715	N/A
Guide tube outer radius, cm	0.6120	N/A
Pellet density, g/cm^3 (UO$_2$/MOX)	10.226 / 10.204 [b]	10.02/10.02
System pressure, bar	155	155
Average coolant temperature, K	580 [c]	584.95
Coolant average density, g/cm^3	0.7116	0.700594
Power, MW (thermal/electric)	3800 / 1300 [a]	3800 / 1300 [a]
Number of Fuel assemblies	193 [a]	193 [a]
Specific power density, W/g	36.0548 [d]	36.0548 [d]

a) Values given in Table 4 of Reference 1.
b) Calculated by the heavy metal mass of the Table 4 of Ref. 1:

$$\rho = \frac{M_{HM}}{(\pi r_p^2 \times h \times n_r \times w_{HM})}$$

M_{HM} = mass of heavy metal per assembly

r_p = pellet radius

h = active height of fuel rod

n_r = number of fuel rods per assembly

w_{HM} = mass fraction in a heavy metal dioxide

c) Assumed as the PWR operating conditions.
d) Calculated by the given power and mass of heavy metal in Ref. 1.

3. Methodologies for Pu Multi-Recycling in the CORAIL Assembly

3.1. WIMS8a Code for the Assembly Calculations

Although significant spatial dependencies are present in a PWR core, 2-dimensional, assembly-level calculations are adequate for the present scoping study of the heavy metal mass flows which result from Pu multi-recycling in a CORAIL fueled core. Previous work demonstrated good agreement between assembly-level and whole core analyses for calculating discharge heavy metal isotopic fractions in a homogenous MOX assembly.

The WIMS8a code,[6] a well-developed neutron transport code capable of calculating neutron fluxes, reaction rates, and the eigenvalue for a lattice geometry problem, was selected for the assembly-level calculations. A 172-group neutron cross section library based on JEF2.2 is available to properly account for the self-shielding of the thermal and epi-thermal energy resonances of the higher actinide isotopes (particularly Pu-242). The neutron transport equations were solved using a characteristics method (CACTUS module), which is one of many transport solution techniques available in the WIMS8a code. It was found that condensing the cross section data to 28 groups prior to the transport calculation provided a significant improvement in computational speed with little penalty on the solution accuracy. The full sequence of WIMS8a modules utilized is provided in Reference 2.

The code is capable of estimating the time-dependent heavy metal composition (on a pin by pin basis) with good accuracy because it explicitly models the transmutation (including radioactive decay) of heavy metal isotopes from Th-232 to Cm-245. Also, around 100 fission products are explicitly modeled. These account for roughly 99.9% of the neutron capture effect of the fission products, while a "pseudo" fission product is utilized to account for neutron scattering by the fission products.

The heterogeneous fuel pin configuration of the CORAIL assembly causes sharp flux gradients within the assembly, yielding a hot-channel factor that is much larger than that observed in a typical UO_2 (homogenous) fuel assembly. The sensitivity of the hot-channel factor to the uranium enrichment and Pu content in the CORAIL assembly, as well as a constraint on the hot-channel factor (<1.20 in this study), demands a solution method that can accurately calculate the pin power distribution. As a benchmark exercise, the power distribution predicted by WIMS8a was compared with the results of an MCNP4C[7] calculation utilizing ENDF/B-VI data.

The benchmark problem was proposed by the CEA as part of the collaboration work between ANL and CEA. The benchmark specification is presented in Table 3.1, where cases with 8% and 12% plutonium in the MOX pins are considered. Because of limited cross section

evaluations at operating temperatures in the available MCNP4C libraries, the benchmark calculations were performed at room temperature conditions. The MCNP4C calculation tracked 5,000,000 neutron histories; the first 250,000 histories were ignored to allow convergence of the fission source before averaging k_∞ or accumulating the energy deposition tallies from which the pin power distribution was derived. Reflective boundary conditions were applied in the MCNP and WIMS8a calculations.

Comparisons of the k_∞ values and normalized pin power distributions predicted by MCNP4C and WIMS8a are provided in Table 3.2 and Figure 3.1. The WIMS8a power distributions presented in Figure 3.1were calculated with a 28-group transport solution, which is the same group structure as used in the CORAIL assembly level calculations. The k_∞ values and power distributions agree well within the statistical uncertainty of the MCNP4C result. The maximum observed difference in k_∞ is 131 pcm (<0.15% k). The WIMS8a normalized pin powers are generally within $\pm 2\sigma$ of the MCNP result. Slightly larger differences (but still < 2.0%) are observed in a few locations at the interface between the UO_2 and MOX pins. The good agreement of WIMS8a with the Monte Carlo calculation indicates that it is well-suited for predicting the pin power distribution in a heterogeneous lattice. It is anticipated that at operating temperatures, WIMS8a would do just as well at predicting the pin power.

3.2. Linear Reactivity Model to Obtain the Desired Cycle Length

Assembly-level calculations with reflective boundary conditions were utilized to model the performance of a reactor loaded entirely with CORAIL assemblies. For a core loaded with a uniform assembly design in a multi-batch fuel management scheme, the linear reactivity model[5] gives the relationship between the core critical burnup (B_c) and the assembly discharge burnup (B_d):

$$B_c = \frac{n+1}{2n} B_d , \tag{1}$$

where n denotes the number of fuel management batches. Here, the critical burnup is equivalent to the core average burnup at the end of cycle (EOC). As in the CEA studies, a 3 batch core with a cycle length of 15,000 MWD/t was assumed. This yields an assembly discharge burnup of 45,000 MWd/t and, according to Equation 1, a critical burnup of 30,000MWD/t.

Generally, the core fuel loading at beginning of cycle (BOC) is designed such that the effective multiplication factor (k_{eff}) of the core reaches 1.00 when the core average burnup is identical to the critical burnup (in other words, when core reaches the end of cycle). In order to represent the whole core state adequately with an assembly level calculation, the effect of neutron

Table 3.1. Design Specifications for CORAIL Assembly Power Distribution Benchmark.

Assembly pitch, cm	21.6098	
Assembly gap, cm	0.1558	
Fuel		
Fuel pitch, cm	1.2620	
Pellet radius, cm	0.41266	
Atom densities in UO_2 pins (#/barn-cm)		
U-235	1.1315E-3	
U-238	2.1226E-2	
O-16	4.4716E-2	
Atom densities in MOX pins (#/barn-cm)	*8% Pu*	*12% Pu*
Pu-238	6.9723E-5	1.0459E-4
Pu-239	7.2243E-4	1.0837E-3
Pu-240	5.3327E-4	7.9993E-4
Pu-241	2.1750E-4	3.2627E-4
Pu-242	2.0904E-4	3.1358E-4
Am-2341	2.1892E-5	3.2839E-5
U-235	5.2055E-5	4.9794E-5
U-238	2.0508E-2	1.9617E-2
O-16	4.4667E-2	4.4655E-2
Cladding		
Outer radius, cm	0.47436	
Density, g/cc	6.49012	
Atom densities (#/barn-cm)		
Fe-54	8.0198E-6	
Fe-56	1.2682E-4	
Fe-57	3.0420E-6	
Fe-58	3.8716E-7	
Cr-50	3.0764E-6	
Cr-52	5.9257E-5	
Cr-53	6.7185E-6	
Cr-54	1.6690E-6	
O16	2.8737E-04	
Zr	3.9550E-02	
Guide tube		
Inner radius, cm	0.572945	
outer radius, cm	0.613012	
Coolant		
Density, g/cc	0.700	
Atom densities (#/barn-cm)		
H_2O	2.3399E-2	
B-10	4.6584E-6	
B-11	1.8751E-5	
Temperature, ^oK	300	

Table 3.2. Summary of the MCNP4C and WIMS8a Benchmark Calculations.

Case	MCNP4C	WIMS8a		
		Number of group [a]	Difference of k_∞, pcm [b]	RMS of power error [c]
8% Pu	$k_\infty = 1.13667$ ± 30 pcm	6	93	0.54
		28	69	0.78
		172	131	0.75
12% Pu	$k_\infty = 1.15130$ ± 31 pcm	6	-100	0.76
		28	-61	0.78
		172	11	0.75

a) Number of neutron energy groups in the transport solution.
b) Difference of the $k_\infty = 10^5 * (k_\infty^{WIMS} - k_\infty^{MCNP})$, pcm.
c) Root mean square of the relative power error.
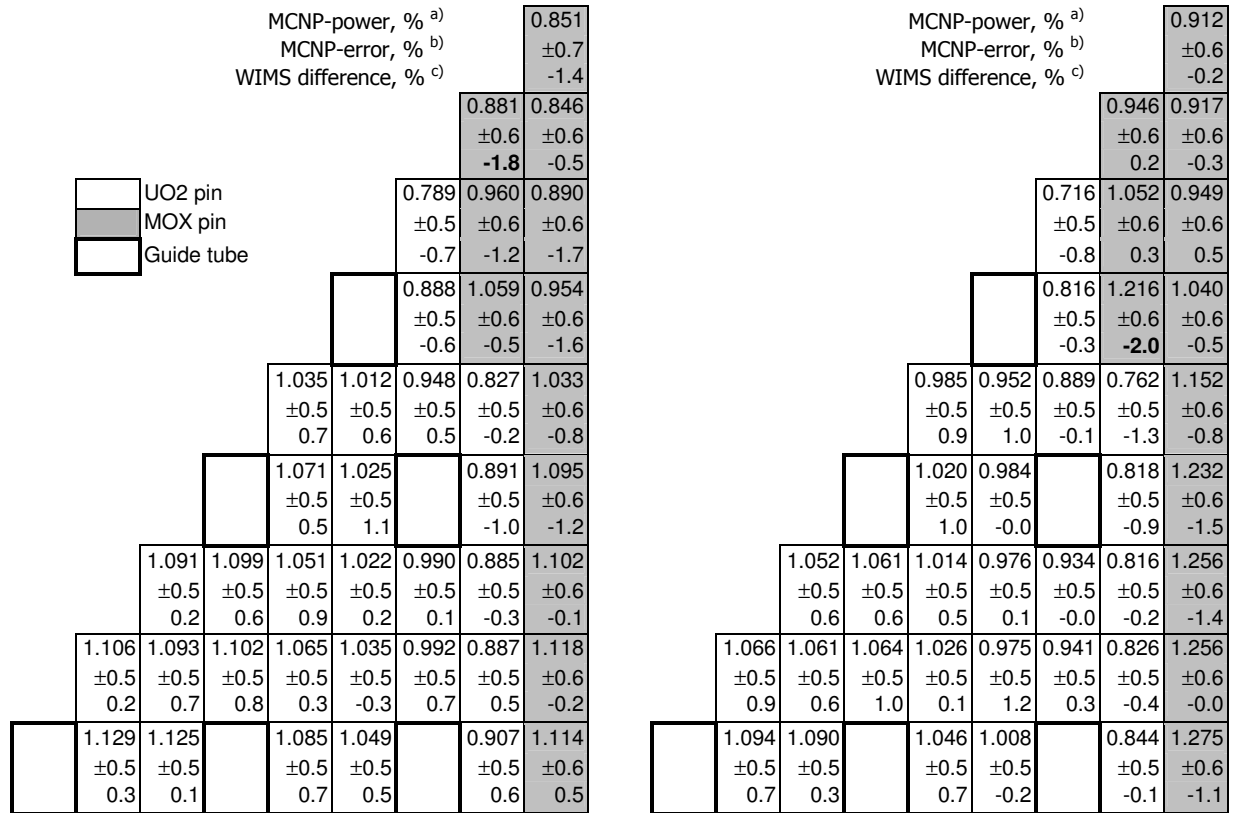
a) The power distribution of MCNP4C derived from the energy deposition tallies
b) The estimated tally relative error
c) % difference between WIMS8a and MCNP4C

(a) **8% Plutonium in MOX fuel**   (b) **12% Plutonium in MOX fuel**

Figure 3.1. Comparison of Normalized Pin Power Distributions Predicted by MCNP4C and WIMS8a for the CORAIL Assembly Benchmark.

leakage through the core boundary must be accounted for in the assembly k_∞ value. In this work, a core leakage of 3% Δk was assumed, based on a WIMS8a eigenvalue calculation of a CORAIL assembly with an EOC composition specified by CEA. Thus, setting the uranium enrichment and Pu content in the CORAIL assembly such that $k_\infty = 1.030$ at the critical burnup will provide a charged assembly loading which meets the desired cycle length for the operating core.

3.3. WIMS8a/ORIGEN2 Coupling Procedure for Evaluation of Radioactive Properties

As the Pu is multi-recycled in the CORAIL assembly, there will be a gradual buildup of higher-mass actinides in the discharged fuel, causing an increase in the radioactive properties (e.g. decay heat, neutron source, radiotoxicity) of the discharged nuclear fuel. These must be evaluated accurately, since higher heat loads can have a negative impact on aqueous fuel processing efficiencies and the increased neutron source may require specific measures to maintain the safety of fuel-handling workers. Also, the long-term impact of discharging the CORAIL assembly to a repository environment must be evaluated.

The ORIGEN2[8] code uses a one-group, point depletion model to solve the equations of nuclide transmutation and decay based on extensive libraries of cross section and decay constant data. One-group cross section data libraries are available for a number of systems, including MOX-fueled lattices, but the capability to utilize problem-specific cross section data is not available. Thus, the extensive libraries available to ORIGEN2 enable an estimate of the mass and radioactivity of all heavy metal and fission product isotopes of practical interest, but the predicted nuclide masses (and intrinsic radioactive properties) at a given fuel burnup are less accurate for cases which are not as well represented with the available generalized cross section data.

On the other hand, WIMS8a uses core-state-dependent cross section data to solve the depletion equations with high accuracy. However, the short-lived (e.g. U-239) and lower- (below Th-232) and higher-mass (above Cm-245) minor actinides are not included in the WIMS8a depletion chains. Additionally, only around 100 individual fission product isotopes are represented in the depletion chains (those that have been determined to be important from a neutronic viewpoint). Thus, a number of nuclides which may be contribute significantly to the radioactive properties of the discharged fuel are not explicitly represented in the WIMS8a models.

In order to obtain more accurate predictions of the radioactive properties of *all* nuclides in the discharged fuel, a procedure to couple the results of ORIGEN2 and WIMS8a was developed. This procedure is displayed graphically in Figure 3.2. To begin, both codes are utilized to predict the isotope masses in 1 metric ton of fuel depleted to the discharge burnup. The isotopes tracked by ORIGEN2 are then classified into two groups, WIMS-isotopes and non-WIMS-isotopes,

10

where the WIMS-isotopes are those that also exist in the WIMS8a depletion chains. In the case of a WIMS-isotope, the concentration predicted by ORIGEN2 is replaced by the result of the WIMS8a code. The concentrations of the non-WIMS-isotopes are then re-normalized to conserve the total masses of the heavy metals and fission products predicted by ORIGEN2. The combined
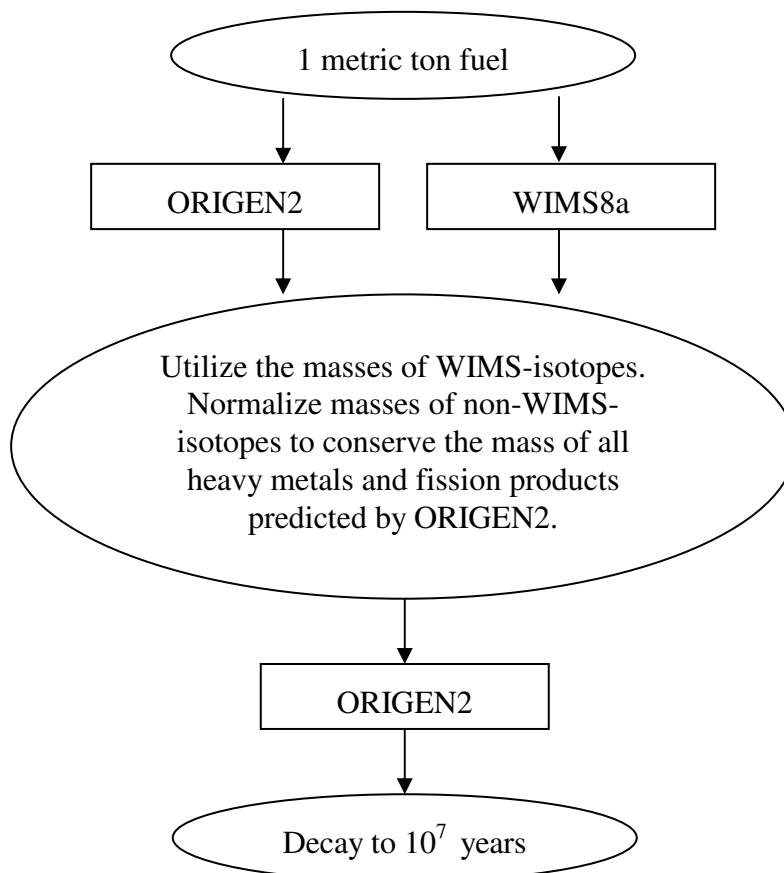

Figure 3.2. The WIMS8a/ORIGEN2 Coupling Procedure to Calculate the Radioactive Properties of Discharged Fuel.

and re-normalized concentrations of *all* nuclides in the lattice at discharge are input to a subsequent ORIGEN2 calculation in order to predict the radioactive properties at discharge and several time points thereafter.

Table 3.3 provides the radiotoxicity (in terms of cancer dose) for 1 metric ton of heavy metal irradiated and discharged from a UO_2 assembly and the CORAIL assembly with Pu multi-recycling. The values in the table are normalized to the radiotoxicity of 5 tons of natural uranium ore (the approximate mass of ore needed to produce 1 ton of low enriched uranium). The notation "*All-HM of CORAIL*" indicates that all heavy metal nuclides discharged from the CORAIL assembly are included in the radiotoxicity evaluation. It should be noted that in the

anticipated recycle scenario of the CORAIL concept (see Section 3.4) only 0.1% of the Pu discharged from the assembly would pass to the repository environment.

Table 3.3. Predictions of Discharged Assembly Radiotoxicity from WIMS8a/ORIGEN2.

		Reference UO$_2$ Assembly [a)]		All-HM of CORAIL	
Decay time		10 year	1000 year	10 year	1000 year
Normalized total radiotoxicity		2561.2	168.0	5312.9	443.9
Correction due to the coupling procedure		-61.2	13.9	-2211.5	32.1
Non-WIMS isotopes	HM	0.0	0.0	0.0	0.0
	FP	1562.3	0.0	1434.5	0.0
	Sum	1562.3	0.0	1434.5	0.0
WIMS isotopes	HM	896.4	168.0	3772.2	443.9
	FP	102.4	0.0	106.3	0.0
	Sum	998.9	168.0	3878.4	443.9

a) Reference UO$_2$ assembly denotes the 4% enriched homogeneous UO$_2$ assembly.

The results in Table 3.3 give an indication of the importance of the WIMS8a/ORIGEN2 coupling procedure for accurately predicting the radiotoxicity of the discharged fuel. The radiotoxicity is much higher for the CORAIL spent fuel due to greater concentrations of plutonium isotopes and other higher actinides (particularly Am-241 and Cm-244) compared with the discharged UO$_2$ assembly. Note also that the "Correction due to the coupling procedure" (which is the difference between the corrected radiotoxicity and that predicted by ORIGEN2 alone) is quite large for the CORAIL assembly. For this case, the ORIGEN2 cross section library for a MOX fueled assembly was utilized, but this, of course, is not particularly applicable to the CORAIL assembly, which is only partially loaded with MOX. Thus, predictions of the radiotoxicity of the discharged CORAIL assembly based on ORIGEN2 alone would be quite inaccurate unless problem-specific cross section data can be utilized. It should be noted that for the UO$_2$ assembly, the generalized cross section data available to ORIGEN2 are quite representative, as indicated by the relatively small radiotoxicity correction.

For the reference UO$_2$ assembly 10 years after discharge, the WIMS-isotopes account for only 39% of the total radiotoxicity, as the fission products not tracked by WIMS8a form a large component of the total. For the CORAIL assembly, however, the WIMS-isotopes account for 73% of the total radiotoxicity. Although the radiotoxicity of the fission products is roughly the same for both the UO$_2$ and CORAIL assemblies, the heavy metal isotopes, which are mostly tracked by WIMS8a, form a larger component of the total radiotoxicity in the CORAIL assembly. After 1000 years, the heavy metal nuclides dominate the radiotoxicity in both cases, which can be sufficiently predicted based on the WIMS-isotopes alone.

3.4. Multi-Recycling Schemes

Figure 3.3 presents a flow diagram for Pu multi-recycling in the CORAIL concept. For a given cycle, the UO_2 and MOX pins in the assembly are fabricated from an external source of enriched uranium and plutonium extracted from the discharge of the previous cycle. A lead-time of two years is assumed from the assembly fabrication to its loading into the reactor. After the assembly is discharged from the reactor, a five year post-irradiation cooling time is allowed before reprocessing the discharged fuel. During reprocessing, it is assumed that 0.1% of the Pu is lost into the waste stream. Additionally, all of the minor actinides (Np, Am, Cm) are removed from the fuel cycle. A companion study investigating the transmutation of this minor actinide stream in a fast-spectrum system is underway.
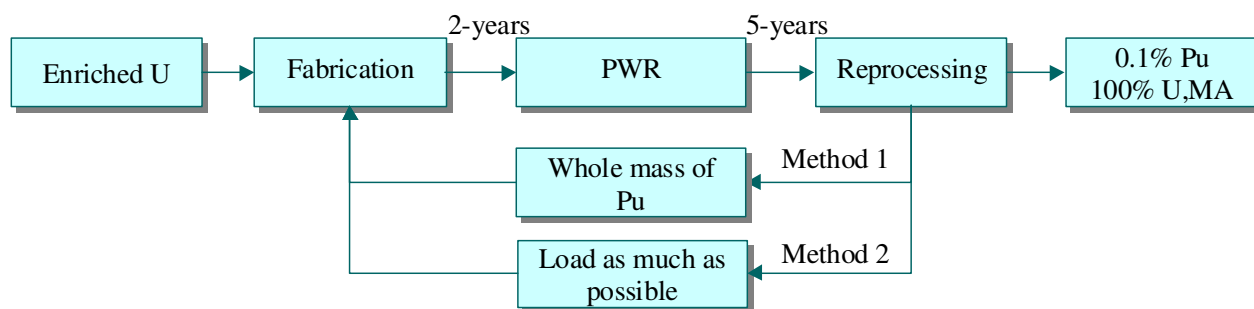

Figure 3.3. Flow Diagram for Pu Multi-Recycling Concepts.

As the Pu isotopic vector changes with each cycle, the "couple" of U enrichment and Pu content in the CORAIL assembly must be determined at the fabrication step, subject to four constraints which were imposed in this study. The first constraint is a cycle length of 15,000 MWD/t, which is met by requiring k_∞ = 1.030 at the critical burnup of 30,000 MWD/t. An enrichment limit of 5 w/o U-235 and a maximum loading of 12% Pu in the MOX pins are two other constraints imposed in this study. A fourth constraint is placed on the hot-channel factor (peak normalized pin power in an assembly), which is limited to 1.2.

As can be seen in Figure 3.3, two methods for determining the couple of uranium enrichment and Pu content were evaluated in this study. In Method-I, which was proposed by CEA originally, the total mass of Pu in the discharged CORAIL assembly (from both the UO_2 and MOX pins) in cycle N is charged in cycle N+1 (after accounting for reprocessing losses). In this scenario, only the uranium enrichment is adjusted to meet the desired cycle length since the Pu content in cycle N+1 is determined by the previous cycle discharge. The plutonium content will likely increase with each successive cycle until the equilibrium state is reached because of the degradation of its fissile content.

If more Pu were loaded in the MOX pins, they would produce a greater share of the total power, increasing the net consumption of Pu in the CORAIL assembly. It is presumed that one way to reach the equilibrium state faster (i.e. with fewer recycles) would be to load as much Pu as possible in the MOX pins, subject to the constraints on the Pu content and the assembly hot-channel factor. This is the approach taken in Method-II. In this method, several couples of uranium enrichment and Pu content that meet the cycle length constraint are considered. The couple with the largest Pu content and yet still meets the constraint on the hot-channel factor is then selected for fabrication. In this scenario, it is possible that the discharge mass of plutonium in cycle N could be less than the specified charge mass in cycle N+1, which would have to be accounted for in the fuel cycle management.

4. Analysis of the CORAIL-Pu Multi-Recycling

4.1. Mass Flow

Multi-recycling of Pu in the CORAIL assembly has been evaluated based on the reprocessing procedures described in Section 3. Cycle-wise results are summarized in Tables 4.1 and 4.2 and Figures 4.1 and 4.2. The startup cycle analysis is discussed in Reference 2. Table 4.3 compares the results at cycle 7 with the multi-recycling results of CEA and a reference UO_2 assembly in a typical once-through fuel cycle. Generally, the results of both Method-I and II are very similar to the CEA results.

Tables 4.1 and 4.2 show that the uranium enrichment progressively increases from 4.15% to 4.57% because of the degradation of the plutonium isotopic vector (decreased fissile content). Similarly, an increase in the plutonium content, from 6.5% to 8.18% in Method-I and to 8.0% in Method-II, is also observed. In the CEA result, the required uranium enrichment is 0.2% higher (at 4.77%), while the plutonium content is 0.4% lower than that predicted by the Method-I approach (which is similar to the CEA approach). It is expected that the CEA result, which is based on a 3-dimensional, whole core analysis, requires the higher uranium enrichment to compensate for other effects missing from the 2-dimensional calculations. Even so, the results from the assembly-level calculations are in fairly good agreement with the whole core analysis performed by CEA. From the cycle-wise results summarized in Table 4.1 and 4.2, it can be seen that the hot-channel factors are below the limiting value of 1.20 from the 1st to the 7th cycle. Note that in all CORAIL cases the hot-channel factors are much higher than that of the reference UO_2 assembly. Burnable absorbers could be used to reduce the hot-channel factor in the CORAIL assembly.

One of the important parameters of interest is the mass balance of the CORAIL-Pu assembly during the multi-recycling. In the 7th cycle, the CORAIL-Pu assembly has a positive Pu mass balance of less than 1.0 kg per assembly, compared with 6.0 kg for the reference UO_2 assembly. On the other hand, the production of minor actinides is larger than for the reference UO_2 assembly, with the mass of minor actinides increasing by roughly 1.2 kg/assembly in the 7th cycle for the CORAIL-Pu assembly, compared to 0.5 kg for the reference UO_2 assembly. In total, the net TRU production is a factor of 3 lower in the CORAIL assembly compared with a reference UO_2 assembly.

4.2. Safety Parameters

Safety parameters for the CORAIL-Pu assembly were evaluated at assembly charge and discharge conditions. The presence of soluble boron, which is used for global reactivity control,

Table 4.1. CORAIL-Pu Multi-Recycling by Method-I.

Cycle			1st	2nd	3rd	4th	5th	6th	7th
U enrichment, %			4.15	4.40	4.48	4.52	4.55	4.56	4.57
Pu-content, %			6.50	6.81	7.16	7.48	7.75	7.98	8.18
Micro. hot-channel			1.175	1.158	1.162	1.165	1.166	1.167	1.169
Initial Plutonium vector		Pu^{238}	2.7	3.06	3.53	3.77	3.86	3.89	3.89
		Pu^{239}	56.0	42.84	39.65	38.25	37.33	36.64	36.06
		Pu^{240}	25.9	30.03	29.32	28.42	27.76	27.29	26.97
		Pu^{241}	7.4	11.81	11.82	11.46	11.17	10.95	10.78
		Pu^{242}	7.3	11.01	14.41	16.88	18.69	20.05	21.14
		Am^{241}	0.7	1.20	1.20	1.16	1.13	1.11	1.09
		Fissile	63.4	54.7	51.5	49.7	48.5	47.6	46.8
Mass (kg/Assembly)	Pu	Charge	11.0	11.4	12.0	12.6	13.0	13.4	13.8
		Discharge	12.0	12.6	13.1	13.6	14.0	14.3	14.6
		Net	1.0	1.2	1.1	1.0	1.0	0.9	0.8
	MA	Charge	0.1	0.1	0.2	0.2	0.2	0.2	0.2
		Discharge	0.9	1.1	1.2	1.2	1.3	1.3	1.4
		Net	0.8	1.0	1.0	1.0	1.1	1.1	1.2
	TRU	Charge	11.1	11.5	12.2	12.8	13.2	13.6	14.0
		Discharge	12.9	13.7	14.3	14.8	15.3	15.6	16.0
		Net	1.8	2.2	2.1	2.0	2.1	2.0	2.0

Table 4.2. CORAIL-Pu Multi-Recycling by Method-II.

Cycle			1st	2nd	3rd	4th	5th	6th	7th
U enrichment, %			4.15	4.33	4.42	4.43	4.49	4.54	4.57
Pu-content, %			6.50	7.30	7.80	8.00	8.00	8.00	8.00
Micro. hot-channel			1.175	1.155	1.153	1.161	1.164	1.165	1.168
Initial Plutonium vector		Pu^{238}	2.7	3.06	3.57	3.85	3.85	3.95	3.96
		Pu^{239}	56.0	42.84	39.22	37.58	37.59	36.70	36.23
		Pu^{240}	25.9	30.03	29.64	28.82	28.81	28.03	27.38
		Pu^{241}	7.4	11.81	11.85	11.49	11.49	11.17	10.93
		Pu^{242}	7.3	11.01	14.45	17.04	17.03	18.94	20.33
		Am^{241}	0.7	1.20	1.20	1.16	1.16	1.13	1.11
		Fissile	63.4	54.7	507	49.1	4.0	47.9	47.5
Mass (kg/assembly)	Pu	Charge	11.0	12.3	13.1	13.1	13.4	13.4	13.4
		Discharge	12.0	13.2	13.9	13.9	14.3	14.3	14.3
		Net	1.0	0.9	0.8	0.5	0.9	0.9	0.9
	MA	Charge	0.1	0.2	0.2	0.2	0.2	0.2	0.2
		Discharge	0.9	1.1	1.2	1.2	1.3	1.3	1.3
		Net	0.8	0.9	1.0	1.0	1.1	1.1	1.1
	TRU	Charge	11.1	12.5	13.3	13.3	13.6	13.6	13.6
		Discharge	12.9	14.3	15.1	15.1	15.6	15.6	15.6
		Net	1.8	1.8	1.8	1.8	2.0	2.0	2.0

Table 4.3 Comparison of Results for Pu Multi-Recycling in the CORAIL Assembly.

Assembly			1st cycle	7th cycle			Reference UO$_2$
				CEA [a]	Method I	Method II	
Assembly Data [b] Neutron Energy group Target k$_\infty$ at 30GWD/t			WH 172/28 1.030	CEA 99 N/A	WH 172/28 1.030	WH 172/28 1.030	WH 69/9 1.044
U Enrichment, % Pu Content, % Micro. Hot-Channel Factor			4.15 6.50 1.196	4.77 7.79 1.14	4.57 8.18 1.169	4.57 8.00 1.168	4.00 - 1.06
Initial Plutonium Vector		^{238}Pu	2.7	4.2	3.9	4.0	
		^{239}Pu	56.0	36.7	36.1	36.2	
		^{240}Pu	25.9	26.8	27.0	27.4	
		^{241}Pu	7.4	11.0	10.8	10.9	
		^{242}Pu	7.3	20.3	21.1	20.3	
		^{241}Am	0.7	1.1	1.1	1.1	
		Fissile	63.4	47.7	46.8	47.5	
Mass Balance (kg/assembly)	Pu	Charge	11.0	13.1	13.8	13.4	0.0
		Discharge [c]	11.7	13.8	14.6	14.3	6.0
		Net	0.7	0.7	0.8	0.9	6.0
	MA	Charge	0.1	0.2	0.2	0.2	0.0
		Discharge	1.1	1.3	1.4	1.3	0.5
		Net	1.0	1.1	1.2	1.1	0.5
	TRU	Charge	11.1	13.3	14.0	13.6	0.0
		Discharge	12.8	15.1	16.0	15.6	6.5
		Net	1.7	1.8	2.0	2.0	6.5
Reactivity Coefficient [d]	Boron Worth (pcm/ppm)	Charge	-5.5	-5.2	-5.3	-5.3	-6.7
		Discharge	-4.0	-6.0	-4.2	-4.3	-9.4
	FTC (pcm/K)	Charge	-2.5	-2.8	-2.4	-2.4	-2.2
		Discharge	-4.6	-3.0	-4.4	-4.4	-3.6
	MTC (pcm/K)	Charge	-15	-19	-16	-17	-3
		Discharge	-63	-63	-66	-66	-72
	Void (pcm/% void)	Charge	N/A	N/A	-243	-244	-259
		Discharge			-527	-529	-693
Neutron source (#/sec) [e]		Discharge 10 year	N/A	N/A	4.60E+09 2.33E+09	N/A	6.60E+08 2.55E+08

a) The CEA results of reference 1, which considered the leakage effect. There is ~0.2% uranium enrichment difference between 2- and 3-dimensional calculations due to the leakage effect.

b) WH and CEA denote the 17x17 Westinghouse and CEA assembly data given in Table 2.1.

c) Discharge burnup is 45 GWD/t.

d) Reactivity coefficients calculated by CEA are at BOC and EOC conditions with critical soluble boron.

e) Spontaneous fission neutron production (neutrons/sec) per assembly at discharge and after 10 years cooling.

was neglected in the assembly-level analyses. The results summarized in Table 4.3 and Figures 4.3 through 4.6 show that the reactivity coefficients are relatively insensitive to the approach used for multi-recycling the Pu (compare the Method-I with Method-II results).   Also, the assembly-level calculations of the reactivity coefficients are in somewhat good agreement with the CEA results, which are based on whole-core analyses at BOC and EOC conditions with a critical soluble boron concentration.

As shown in Figure 4.3, the fuel temperature coefficient of the CORAIL-Pu assembly exhibits a behavior similar to that of the reference UO_2 fuel assembly, with the CORAIL-Pu coefficient being slightly more negative. Figure 4.4 shows that the soluble boron worth of the CORAIL-Pu is less negative than the UO_2 assembly because of the harder spectrum that exists in a Pu-bearing lattice. Because of the lower soluble boron worth, the boron concentration needed to suppress the excess reactivity at BOC will need to be about 20% higher in a CORAIL fueled core. The moderator temperature coefficient (MTC) is strongly dependent on the concentration of soluble boron because of the effective loss of boron (a positive reactivity effect) that occurs as the water density decreases with increasing temperature. This effect is evident in Figure 4.5, in which the MTC values with 1631 ppm soluble boron are less negative than those without soluble boron for both the CORAIL-Pu and UO_2 fuel assemblies. It should be noted that the positive MTC for the UO_2 assembly in Figure 4.5(b) is due to the unusually high soluble boron concentration utilized in this calculation (a UO_2 fueled core will typically have ~1300 ppm at BOC). The control rod worth in the CORAIL concept was approximated by replacing the 24 guide tubes with B_4C rods and comparing the assembly k_∞ for the "all rods in" and "all rods out" condition. From Figure 4.6 it can be seen that compared to a UO_2 assembly, the rod worth is less negative due to the harder spectrum in the CORAIL assembly.
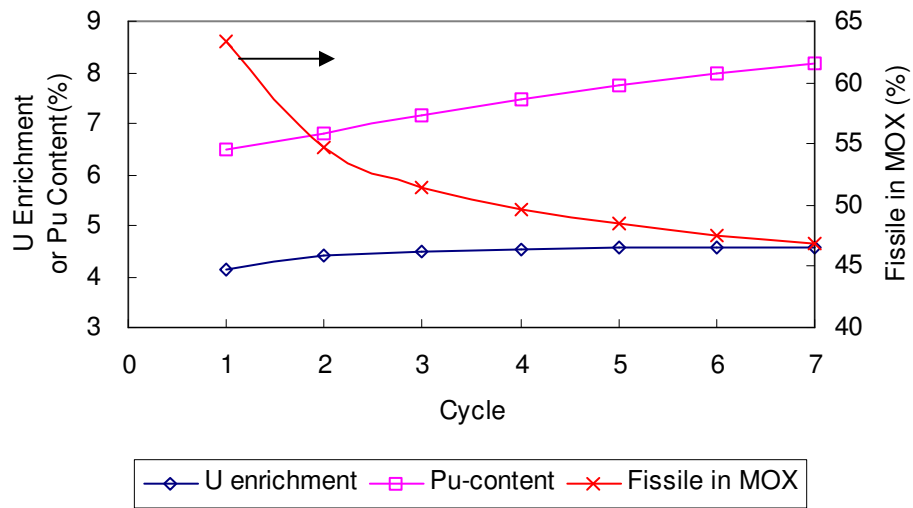
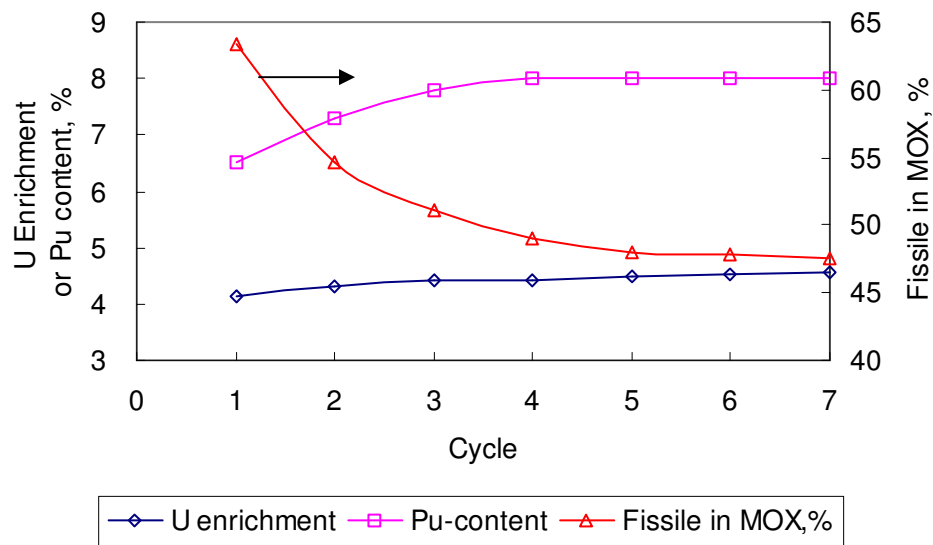**Figure 4.1. The Multi-Recycling of the CORAIL-Pu Assembly with Method-I.**

Figure 4.2. The Multi-Recycling of the CORAIL-Pu Assembly with Method-II.
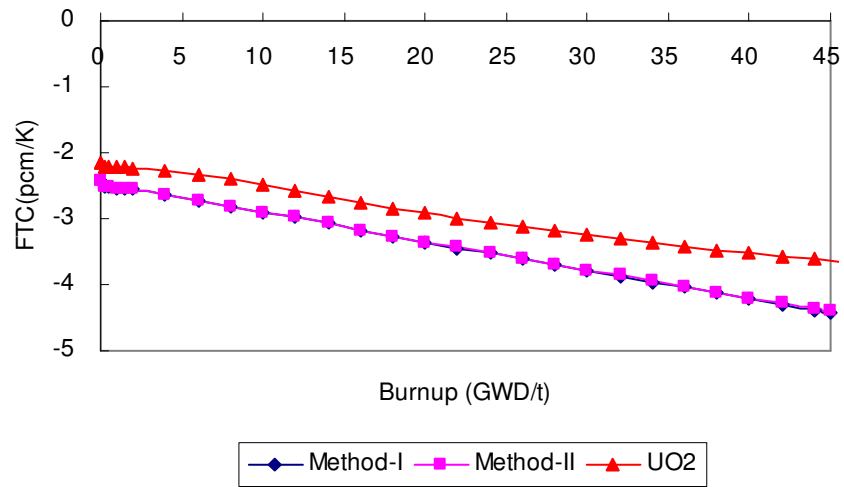
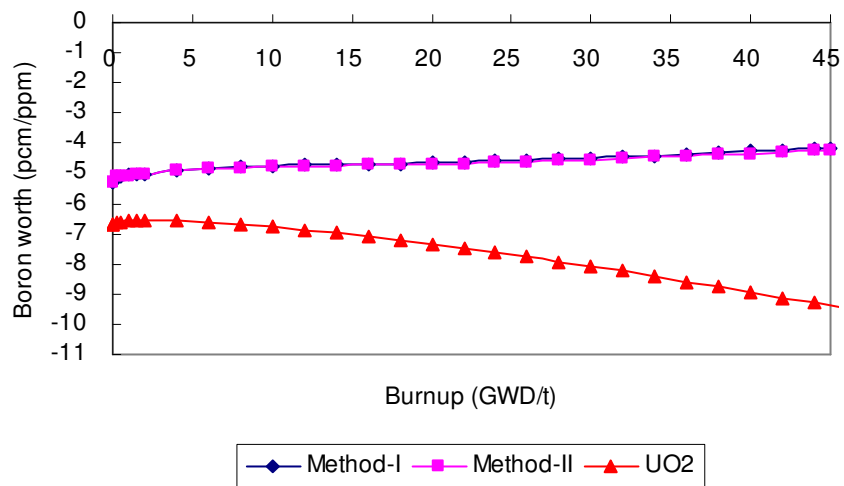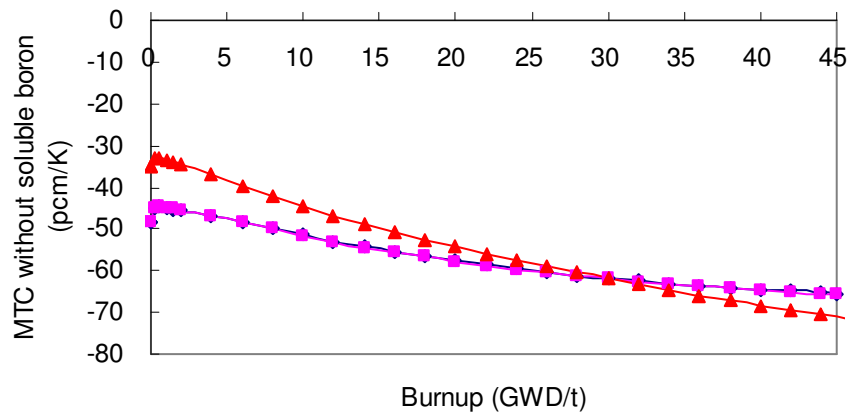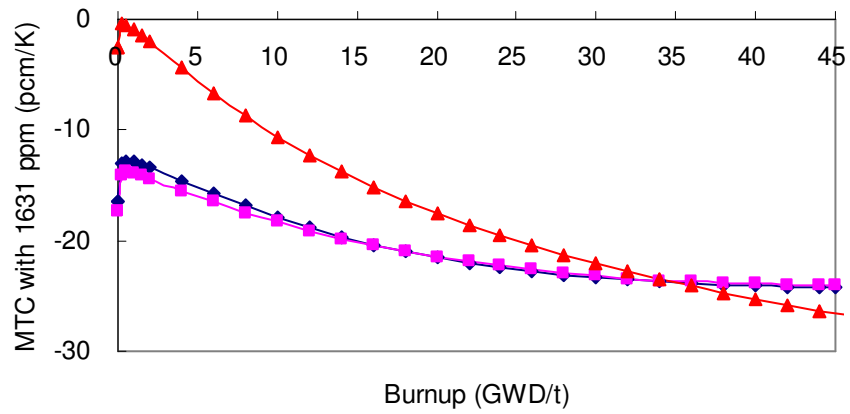**Figure 4.3. Fuel Temperature Coefficient of the CORAIL-Pu Assembly at 7th Cycle.**

Figure 4.4. Soluble Boron Worth of the CORAIL-Pu Assembly at 7th Cycle.

(a) Without Soluble Boron

(b) 1631 ppm Soluble Boron

Figure 4.5. Moderator Temperature Coefficient of the CORAIL-Pu Assembly at 7th Cycle.
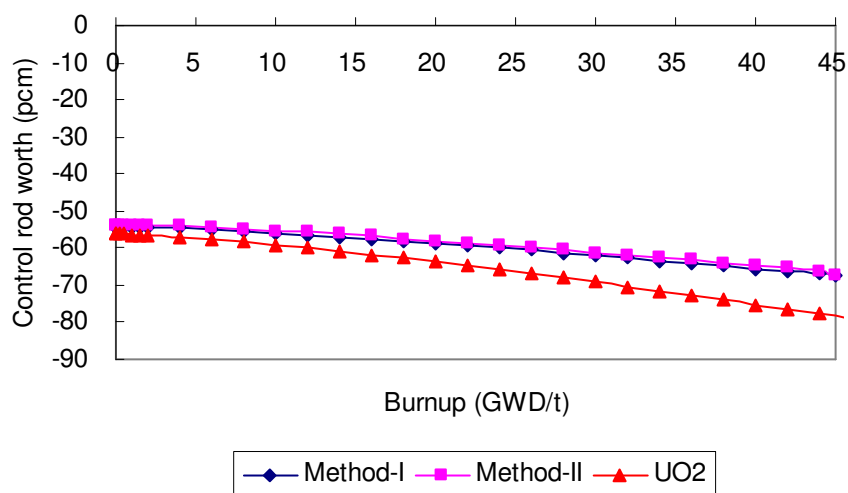
Figure 4.6. Control Rod Worth of the CORAIL-Pu Assembly at 7th Cycle.

4.3. Radiotoxicity

As shown in Figure 3.3, the discharged CORAIL assembly is processed after a 5 year cooling interval, with 99.9% of the Pu being recovered and kept within the reactor fuel cycle. In the present study, it was assumed that 0.1% of the Pu, plus all the minor actinides (Np, Am, Cm) and fission products enter into long-term storage in a repository environment; the discharged uranium could be used as a makeup feed or stored as low-level waste. On the other hand, it was assumed that *all* of the heavy metal and fission product nuclides discharged from the reference UO_2 assembly (again, following 5 years cooling) are stored in a repository, since partitioning of the once-through, spent UO_2 fuel would not be practiced.

A variety of measures are available to quantify the *radiotoxicity* of spent nuclear fuel. These *hazard* measures assess the consequence of exposure to the radiation sources; thus, they do not comprise a *risk* analysis, which would need to account for radionuclide release and transport. Because food or water contamination is the most likely mechanism for repository release, ingestion measures are preferred. For this study, two commonly used hazard measures were considered: dose equivalent derived from the ICRP database[9] and water dilution volume from *10CFR20*[10]. For consistency with international studies and recent biological radiation studies, the cancer dose measure is recommended for future comparisons. This measure was solely utilized in the FY01 multiple strata study[11]. The precise technique employed to generate the dose factors is described in Reference 12.

The radiotoxicity *discharged to waste* from 1 metric ton of discharged CORAIL and UO_2 fuel, expressed in terms of the cancer dose and the water dilution hazard, was evaluated for up to

10 million years after disposal. These radiotoxicity measures are provided in Figures 4.7 and 4.8, respectively, with a comparison made between the CORAIL and the reference UO_2 assemblies. Each radiotoxicity measurement is normalized to the amount of natural uranium ore needed to fuel an enriched UO_2 assembly (assumed to be 5 tons of natural uranium to produce 1 ton of enriched uranium).

Similar trends are observed for both the cancer dose and the water dilution hazard. The radiotoxicity levels of the spent nuclear fuel sent to the repository environment from the CORAIL and UO_2 assemblies are initially about the same, but after a few hundred years the radiotoxicity of the CORAIL discharge is a factor of two or more lower. Consequently, the ingested cancer dose falls below that of the uranium ore (normalized toxicity = 1.0) much sooner in the case of the CORAIL assembly, although this still requires ~30,000 years storage time to allow for the decay of the minor actinides. A companion study, in which the minor actinides from the CORAIL assembly enter into a fast-spectrum transmutation system, is under way.

Table 4.4 summarizes the 10 leading contributors to the cancer dose from the material stored in the repository at 10, 1000, 100,000, and 1,000,000 years after initial storage. Similarly, Figure 4.9 shows the time-dependant behavior of some of the leading isotopic contributors to the ingested cancer dose over 10^7 years in the repository. At 10 years, the radiotoxicity of the CORAIL assembly discharge is 12% higher than the UO_2 assembly discharge due to higher concentrations of Cm-244 and other minor actinides. Recall from Table 4.3 that the discharge mass of minor actinides is 2-3 times higher for the CORAIL assembly. However, since 99.9% of the Pu stays in the reactor fuel cycle, the contribution of the Pu isotopes to the radiotoxicity in the repository is only 0.2%, compared with 23.2% in the discharged UO_2 assembly. It is the near-elimination of the Pu from the repository that yields the long-term reduction in the radiotoxicity of the repository inventory.

The leading contributor to the radiotoxicity at 1000 years is Am-241. While the discharged CORAIL assembly has ~50% more Am-241 than the UO_2 assembly at 10 years, the production of Am-241 (as seen by the rise of the Am-241 contribution from 10 to 100 years in the UO_2 case) from β^- decay of Pu-241 (14.4 year half-life) is practically eliminated. Further, the concentrations of Pu-239 and Pu-240 have also been greatly reduced, so that the cancer doses at 1000 and 100,000 years are factors of 2 and 5 lower due to the multi-recycling of Pu in the CORAIL assembly.

Figure 4.9 also shows that Np-237 is produced in the repository, this coming from the decay of Am-241 (432.7 year half-life). The amount of Np-237 production is seen to be somewhat smaller in the CORAIL case, ultimately due to the reduction of the Pu-241 inventory in the repository. Although Np-237 makes only a very small contribution to the cancer dose in these calculations, this isotope is an important concern because it will more readily transport out

of the repository in the event of failed storage casks. Pu multi-recycling in the CORAIL assembly reduces the Np-237 inventory in the repository from 1000 to 10^6 years by ~30%.
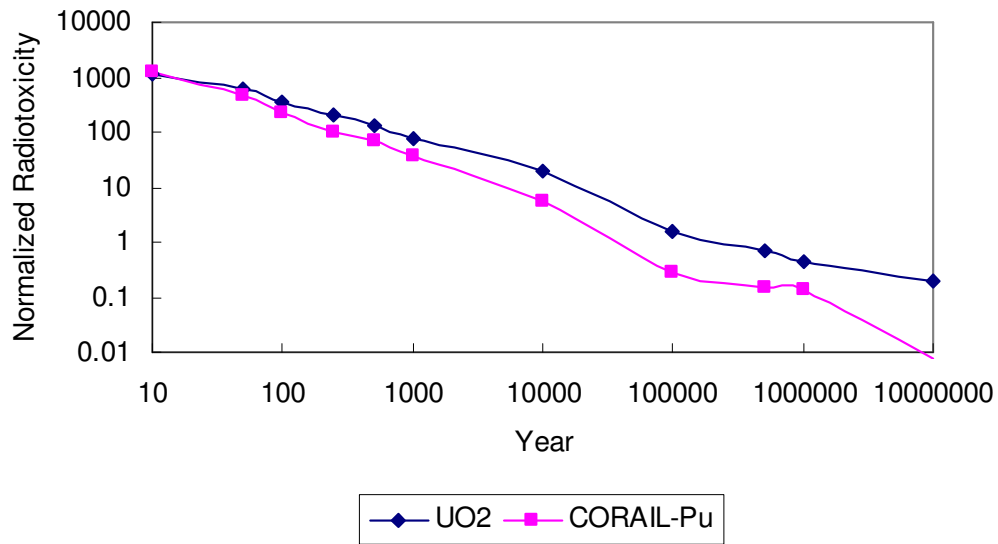
Figure 4.7. Radiotoxicity of Repository Waste (in Terms of the Cancer Dose Hazard) from Spent Fuel Discharged from the UO$_2$ and CORAIL-Pu Assemblies.
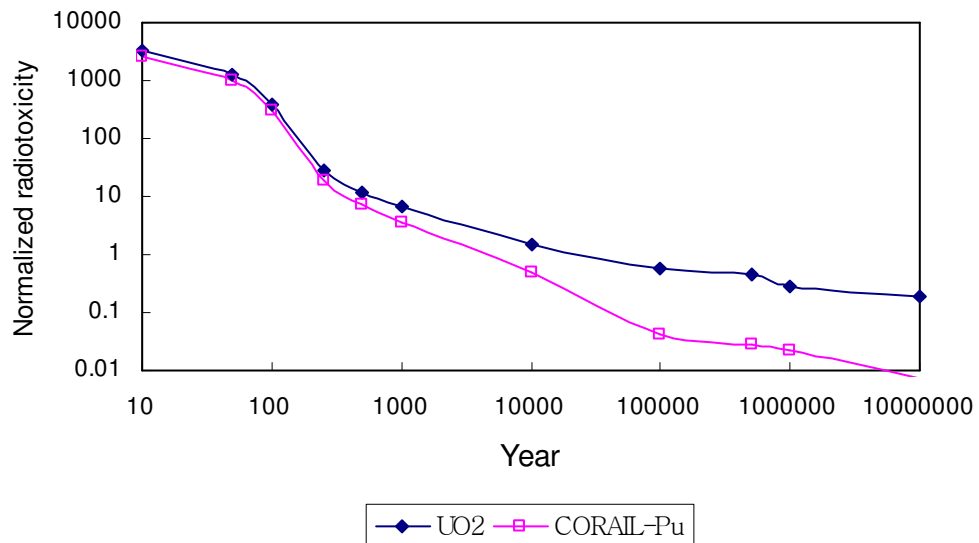

Figure 4.8. Water Dilution Hazard for Repository Waste from Spent Fuel Discharged from the UO$_2$ and CORAIL-Pu Assemblies.

Table 4.4 Leading Contributors to Cancer Dose.

	UO$_2$ Assembly					CORAIL assembly			
	Years after discharge					Years after discharge			
	10	1,000	100,000	1x10^6		10	1,000	100,000	1x10^6
Sr-90	358.92				Cm-244	499.51			
Cs-137	269.01				Sr-90	287.56			
Pu-238	149.74				Cs-137	271.95			
Am-241	86.96				Am-241	131.55			
Pu-241	70.76				Y-90	46.02			
Cm-244	63.01				Am-243	6.76			
Y-90	57.44				Cs-134	6.38			
Pu-240	24.22				Cm-243	3.38			
Cs-134	19.81				Eu-154	2.66			
Pu-239	14.94				Am-242m	1.57			
Sum	1121.00				Sum	1261.38			
Pu/Total, %	23.2				Pu/Total, %	0.2			
Am-241		39.95			Am-241		27.18		
Pu-240		22.12			Am-243		6.16		
Pu-239		14.56			Pu-240		3.64		
Am-243		0.96			Cm-245		0.30		
Pu-242		0.10			Pu-239		0.25		
Pu-238		0.06			Cm-246		0.20		
Np-237		0.03			Np-239		0.04		
Cm-245		0.02			Pu-238		0.04		
U-234		0.02			Np-237		0.02		
Np-239		0.01			Am-242m		0.02		
Sum		77.85			Sum		37.85		
Pu/Total, %		47.3			Pu/Total, %		10.4		
Pu-239			0.87		Pu-239			0.20	
Po-210			0.26		Th-229			0.04	
Pb-210			0.12		Np-237			0.02	
Pu-242			0.08		Ra-225			0.01	
Th-229			0.05		Po-210			0.01	
Ra-226			0.05		U-233			0.00	
Th-230			0.03		Pu-242			0.00	
Np-237			0.03		Ac-225			0.00	
U-234			0.01		Tc-99			0.00	
Ra-225			0.01		Pb-210			0.00	
Sum			1.55		Sum			0.29	
Pu/Total, %			61.6		Pu/Total, %			69.5	
Po-210				0.13	Th-229				0.08
Th-229				0.11	Ra-225				0.02
Pb-210				0.06	Np-237				0.02
Ra-226				0.02	U-233				0.01
Ra-225				0.02	Ac-225				0.01
Np-237				0.02	Po-210				0.00
Pu-242				0.02	Pu-242				0.00
Th-230				0.02	Ac-227				0.00
U-233				0.01	Pb-210				0.00
Ac-225				0.01	Pa-231				0.00
Sum				0.45	Sum				0.14
Pu/Total, %				3.7	Pu/Total, %				0.5
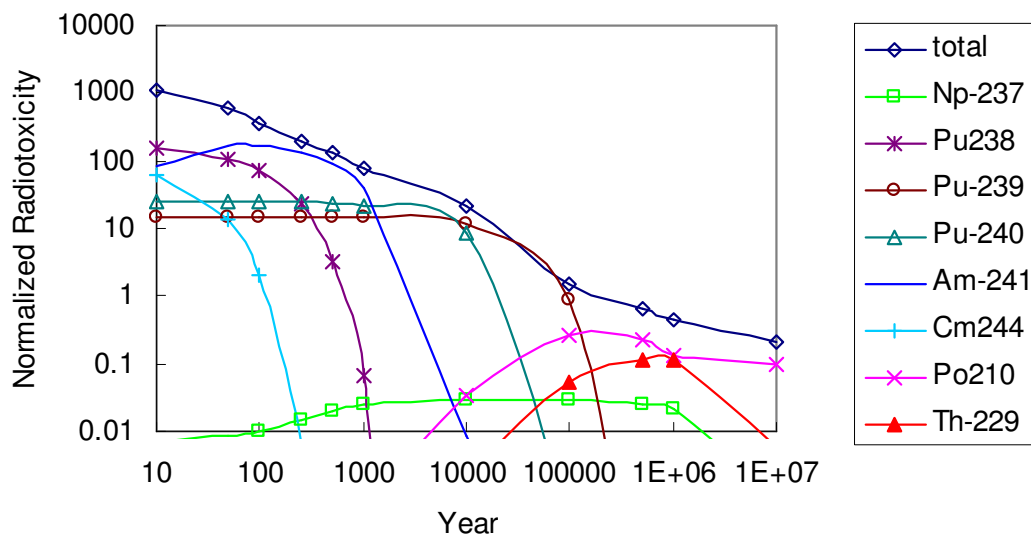
(a) UO2 Assembly
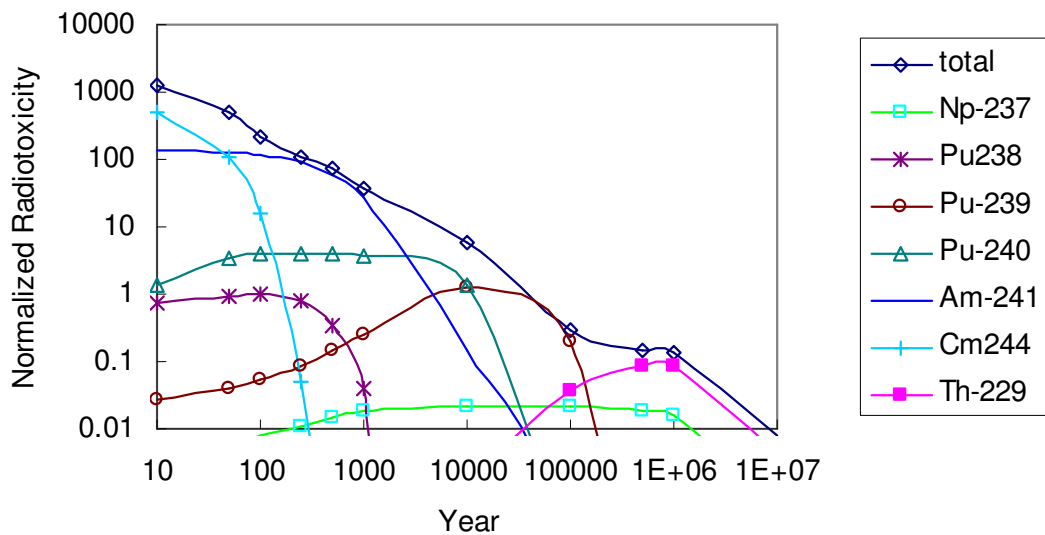
(b) CORAIL-Pu Assembly

Figure 4.9. Isotopic Breakdown of the Cancer Dose Hazard.

5. Conclusions

The multi-recycling of Pu in the CORAIL assembly was assessed with the WIMS8a and ORIGEN2 codes. Results similar to those reported by CEA were obtained utilizing two different multi-recycling approaches. The Pu content stabilizes around 8% and the U-235 enrichment at 4.57% for a 3 batch fuel management scheme and a 15,000 MWD/t cycle length. While a typical UO_2 fueled assembly produces about 6 kg of Pu/assembly, it was found that the CORAIL assembly can achieve an almost zero Pu mass balance (e.g., less than 0.9 kg per assembly at cycle 7) between charge and discharge, without any particular adverse effects on the reactivity coefficients. However, an increased utilization of burnable absorbers may be needed to flatten the pin power distribution in the heterogeneously loaded CORAIL assembly. Pu multi-recycling in the CORAIL assembly reduces the long-term cancer dose radiotoxicity relative to the reference UO_2 assembly by a factor of 2-5. However, eliminating, or greatly reducing, the minor actinide inventory in the repository through TRU multi-recycling in the CORAIL assembly or minor actinide transmutation in a fast-spectrum system will greatly benefit the repository environment.

References

1. G. Youinou, et al, *Heterogeneous Assembly for Plutonium Multi-recycling in PWRs: The CORAIL Concept*, GLOBAL 2001, Paris, France.

2. T. K. Kim, *Analysis of CORAIL Assembly with WIMS8a Code*, Intra-Laboratory Memo, Argonne National Laboratory, November 26, 2001.

3. Nuclear Energy Agency Working Group, *Plutonium Fuel: An Assessment*, NEA-OECD Report, Paris, France (1989).

4. Fuel Review: Design Data, *Nuclear Engineering International*.

5. M. J. Driscoll, et al, *The Linear Reactivity Model for Nuclear Fuel Management*, American Nuclear Society, 1990

6. *WIMS – A Modular Scheme for Neutronics Calculations*, AEA Technology.

7. "MCNP4C, Monte Carlo N-Particle Transport Code System," Los Alamos National Laboratory.

8. A.G. Croff, *ORIGEN2- A Revised and Updated Version of the Oak Ridge Isotope Generation and Depletion Code*, Oak Ridge National Laboratory, ORNL-5621.

9. *Age-Dependent Doses to Members of the Public from Intake of Radionuclides: Part 5 Compilation of Ingestion and Inhalation Dose Coefficients*, ICRP Publication 72, Annals of the ICRP, **26**, No. 1.

10. Code of Federal Regulations, 10CFR20 (rev. 1990).

11. *Candidate Approaches for an Integrated Nuclear Waste Management Strategy – Scoping Evaluations*, AAA-PDO-GEN-01-0051, November, 2001 (Revised).

12. E.E. Morris, *Dose Factors for Estimating Cancer Deaths Resulting from Ingestion of Radionuclides*, Intra-Laboratory Memo, Argonne National Laboratory, June 5, 2002.